

# Investigation of Solvent Isotope Effects on Raman and Fluorescence Intensity of LDS750 in CH<sub>3</sub>OH and CD<sub>3</sub>OD

Fritz J. Knorr, Mark H. Wall, and Jeanne L. McHale\*

Department of Chemistry, University of Idaho, Moscow, Idaho 83844-2343

Received: June 8, 2000; In Final Form: August 8, 2000

The resonance Raman spectra of LDS750 in methanol-*h*<sub>4</sub> and methanol-*d*<sub>4</sub> have been determined at excitation wavelengths on the blue side of the absorption maximum. In contrast to our previous studies of the solvatochromic molecule betaine-30, Raman intensities of LDS750 are observed to be independent of solvent isotopomer. The fluorescence quantum yield, however, was significantly larger in methanol-*d*<sub>4</sub> than in methanol-*h*<sub>4</sub>. The results suggest that the dephasing dynamics that determine the resonance Raman intensities are dominated by intramolecular relaxation rather than solvent motion. Excited-state population relaxation, on the other hand, is perturbed by solvent isotope and the more intense emission in deuterated solvent is a consequence of less favorable Franck–Condon factors for radiationless decay. The radiative lifetime calculated from the quantum yield and fluorescence lifetime is considerably longer than that found using the Strickler–Berg equation, suggesting that the transition moment in the relaxed geometry is reduced from that in the Franck–Condon geometry. Our conclusions concerning excited state dynamics in LDS750 are compared with those obtained from time-domain measurements on this dye.

## 1. Introduction

Recent experimental developments have enabled the observation of solvent relaxation dynamics taking place on a subpicosecond time scale.<sup>1–6</sup> At the same time, there is considerable interest in elucidating the role of solvent dynamics on the rate of fundamental chemical reactions such as electron transfer.<sup>7–10</sup> Analysis of resonance Raman (RR) excitation profiles can provide a window on ultrafast solvent relaxation dynamics through the influence of solvent dephasing on RR intensities. In previous RR studies<sup>11,12</sup> of the solvatochromic molecule betaine-30, we have shown that the subpicosecond inertial solvent relaxation exerts a strong influence on RR intensities. The RR spectra of the chromophore were observed in methanol and acetonitrile and their perdeuterated derivatives, and intensities were generally higher in CH<sub>3</sub>CN than in CD<sub>3</sub>CN, but lower in CH<sub>3</sub>OH compared with CD<sub>3</sub>OD. The results were interpreted by recognizing the very sensitive dependence of Raman intensities on the amplitude of the solvent motion that causes pure dephasing; that is, fluctuations in the electronic transition frequency. The difference in the direction of the intensity change with deuteration in the two solvents derives from the role of collisions in limiting the amplitude of solvent relaxation in acetonitrile versus the overriding influence of hydrogen-bond dynamics in methanol solution.

In a related study, we investigated isotope effects on the Raman intensity of a hemicyanine dye in aqueous solution.<sup>13,14</sup> In that system, different normal modes of the dye were differently perturbed when the solvent H<sub>2</sub>O was replaced by D<sub>2</sub>O. We concluded that these results reflect mode-specific relaxation dynamics, and perhaps direct coupling of solute vibrations to solvent relaxation. Neither of these effects can be quantitatively accounted for within the standard working equa-

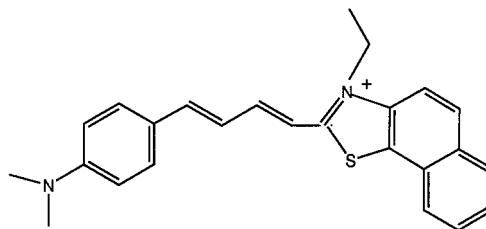


Figure 1. Structure of LDS750.

tions for interpreting RR profiles,<sup>15–20</sup> which are based on the assumption that dephasing and population relaxation are independent of vibrational mode and vibrational state.

Before revised theoretical approaches can be proposed, it is necessary to further elucidate the basis of the solvent isotope effect (SIE) on RR intensities. In the betaine-30 studies, the SIE on RR intensities is closely connected to solvatochromism, which is a consequence of the large difference in the ground- and excited-state dipole moments. Mode-dependent SIEs on the RR intensity, on the other hand, imply that different vibrational modes project out different parts of the solvent spectral density, or that mode-specific relaxation dynamics contribute to the Raman intensity. Such effects would not necessarily be limited to solvatochromic dyes. A further possible contributor to the Raman SIE is the dependence of the excited-state population relaxation on solvent isotope. Radiationless decay rates have been observed to depend on solvent isotope.<sup>22,23</sup>

In this study, we compare the absorption, RR, and fluorescence spectra of LDS750 (Figure 1) in methanol-*h*<sub>4</sub> and methanol-*d*<sub>4</sub>. The moderately large Stokes shift of LDS750 (3200 cm<sup>-1</sup> in methanol) permits the Raman spectra to be excited at wavelengths on the blue side of the absorption maximum; the Raman intensities are observed on top of the fluorescence background (Figure 2). More than 20 normal

\* Author to whom correspondence should be sent (e-mail: jmchale@uidaho.edu).

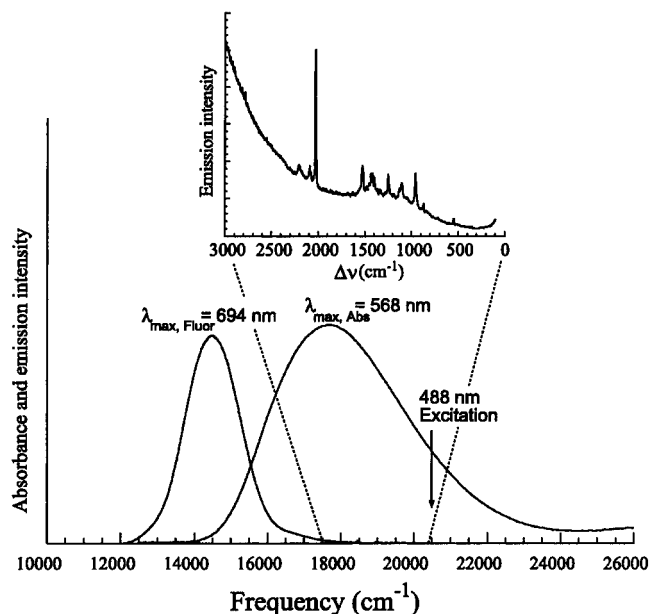


**Figure 2.** Absorption, resonance Raman, and fluorescence spectra of LDS750 in  $\text{CD}_3\text{OD}$ .

modes of LDS750 are coupled to the visible electronic transition, providing ample opportunity for uncovering possible mode-dependent SIEs. LDS750 is much less solvatochromic than betaine-30, enabling us to explore the possible link between nonlinear solvent dynamics and SIEs on RR intensities. For comparison, the absorption maximum of betaine-30 shifts  $\sim 9000\text{ cm}^{-1}$  to the blue, whereas that of LDS750 increases by  $2000\text{ cm}^{-1}$  on going from tetrahydrofuran to water solvent. The fluorescence spectrum of LDS750 is narrower and less sensitive to solvent polarity than the absorption spectrum, suggesting that in the relaxed geometry, the ground and excited state charge distributions are similar. This result is similar to what was observed for the structurally similar hemicyanine dye previously studied in our lab.<sup>13,14</sup>

LDS750 in several solvents was the subject of an early time-dependent fluorescence Stokes shift (TDFSS) study.<sup>24</sup> Fleming and co-workers<sup>25,26</sup> observed a 70 fs component in the TDFSS measurements of LDS750 in acetonitrile, which they assigned to inertial solvent relaxation. LDS750 has also been studied on a femtosecond time scale with four-wave mixing spectroscopy.<sup>27</sup> Blanchard<sup>28</sup> observed inhomogeneous relaxation kinetics in the time-resolved stimulated emission of LDS750, attributed to internal rotation in the excited electronic state. The lack of mirror symmetry in the absorption and fluorescence emission spectra also suggests excited-state isomerization. Ruthmann et al.<sup>29</sup> assigned a 70 fs process in the transient spectrum of LDS750 to intramolecular relaxation, and attributed relaxation in the range  $\sim 200\text{--}600\text{ fs}$  to solvent-dependent isomerization. Lian et al.<sup>30</sup> observed transient changes in the solvent infrared (IR) spectra following excitation of LDS750 to the S1 state, and assigned these changes to the effect of the local field of LDS750 on molecules in the first solvation sphere. Recently, Bardeen et al.<sup>31</sup> studied ultrafast dynamics of LDS750 using time-resolved four-wave mixing. They observed a fast ( $<100\text{ fs}$ ) solvent-independent spectral diffusion process and concluded that intramolecular vibrational relaxation contributed to the sub-100 fs dephasing. A recent femtosecond Stokes shift study of LDS750 in aniline<sup>32</sup> concluded that the sub-100 fs Stokes shift reflects solvation as well as changes in solute conformation, and that these factors are coupled. It is now appreciated that the subpicosecond regime reflects intramolecular dynamics of

LDS750 as well as solvent relaxation, but there remain many questions concerning the exact nature of this early time response. Interpretation of ultrafast spectroscopy experiments that probe chromophore-solvent dynamics is often complicated by the uncertain contribution of vibrational relaxation along with the solvent response.<sup>33</sup> Resonance Raman intensities depend on the same subpicosecond dynamics that show up in these time-domain experiments and provide the opportunity to address this question.

## 2. Experimental Section

LDS750 was purchased from Exciton and used as received. Spectral grade methanol- $\text{d}_4$  was used as received, but methanol- $\text{d}_4$  had to be distilled to remove trace fluorescent impurities. Raman spectra were recorded for solutions containing  $1.45 \times 10^{-4}\text{ M}$  LDS750. Raman spectra were excited with argon ion laser lines at 514.5, 501.8, 488.0, and 457.9 nm, with  $\sim 100\text{ mW}$  of power at the sample, and recorded using a Spex 270 M monochromator with a liquid-nitrogen cooled charge-coupled device (CCD) detector. Solutions were circulated through a capillary sample holder using a syringe pump, and  $90^\circ$  scattering geometry was employed. The fluorescence background was subtracted after fitting it to a fifth-order polynomial. No attempt was made to correct for self-absorption, which was estimated to be  $<5\%$ . The frequency of the solvent standard peak at  $1033\text{ cm}^{-1}$  in  $\text{CH}_3\text{OH}$  is close enough to the  $978\text{ cm}^{-1}$  line used as a standard in  $\text{CD}_3\text{OD}$  to neglect the effect of differential self-absorption in scaling the spectra. Depolarization ratios of LDS750 lines were  $1/3$  to within the error of the measurement. Raman intensities of  $\text{CH}_3\text{OH}$  and  $\text{CD}_3\text{OD}$  were determined relative to the  $802\text{ cm}^{-1}$  line of cyclohexane in binary mixtures containing 0.03 mole fraction cyclohexane in methanol. These intensities were integrated over the range  $800\text{--}1200\text{ cm}^{-1}$  and converted to cross-sections using net depolarization ratios in this range of 0.37 for  $\text{CD}_3\text{OD}$  and 0.25 for  $\text{CH}_3\text{OH}$ . Fluorescence spectra were recorded using the same instrumentation as for the Raman measurements, using more dilute solutions of LDS750 and shorter exposure times. Fluorescence quantum yields ( $\varphi_f$ ) at an excitation wavelength of 568 nm, provided by an argon ion pumped dye laser, were measured relative to cresyl violet in methanol- $\text{d}_4$ , using a reported value of  $\varphi_f = 0.54 \pm 0.03$  for the standard.<sup>34</sup> Fluorescence and Raman spectra were corrected for the instrument response, which was determined using a standard tungsten lamp. The Raman spectrum shown in the inset of Figure 2 was recorded using a scanning double monochromator and photomultiplier tube detection.

## 3. Results

**3.1. Absorption and Emission of LDS750 in  $\text{CH}_3\text{OH}$  and  $\text{CD}_3\text{OD}$ .** Figure 2 shows the absorption and emission spectra of LDS750 in methanol- $\text{d}_4$ , along with the Raman spectrum excited at 488 nm. The absorption spectrum ( $\epsilon_{\text{max}} = 3.57 \times 10^4\text{ L/mol cm}$  at 568 nm) was found to be independent of solvent isotopomer to within the error of the measurement. The shape of the fluorescence spectrum was observed to be independent of excitation wavelength, which is in agreement with previous reports,<sup>28,31</sup> and the same in  $\text{CH}_3\text{OH}$  and  $\text{CD}_3\text{OD}$ . The overall fluorescence intensity, however, is higher in deuterio-methanol than in protio-methanol, at all excitation wavelengths. The fluorescence quantum yield, shown in Table 1 was measured at an excitation wavelength of 568 nm. The 0–0 energy of  $15\,300\text{ cm}^{-1}$  was determined from the intersection of appropriately scaled absorption and fluorescence spectra. Table 1 lists the fluorescence lifetimes,  $\tau_f$ , in both methanol (230 ps)

**TABLE 1: 0–0 Energy,  $E_0$ , Fluorescence Anisotropy,  $r$ , Quantum Yield,  $\varphi_f$ , and Fluorescence Lifetime,  $\tau_f$ , of LDS750 in Methanol and Deuterated Methanol**

solution	$E_0$ , cm <sup>-1</sup>	$r$	$\varphi_f$	$\tau_f$ , ps
LDS750 in CH <sub>3</sub> OH	15 300	0.11 ± 0.01	(4.0 ± 0.2) × 10 <sup>-3</sup>	230 <sup>a</sup>
LDS750 in CD <sub>3</sub> OD	15 300	0.11 ± 0.01	(5.2 ± 0.3) × 10 <sup>-3</sup>	300 <sup>b</sup>

<sup>a</sup> From ref 24. <sup>b</sup> This work, from  $\tau_f = \varphi_f \tau_{\text{rad}}$ .

**TABLE 2: Absorption and Fluorescence Peak Frequency,  $\tilde{\nu}_{\text{max}}$ , Full width at Half-Maximum,  $\Delta\tilde{\nu}_{1/2}$ , and Transition Moment,  $\mu_{\text{ge}}$ , for LDS750 in Methanol**

parameter	$\tilde{\nu}_{\text{max}}$ , cm <sup>-1</sup>	$\Delta\tilde{\nu}_{1/2}$ , cm <sup>-1</sup>	$\mu_{\text{ge}}$ , Debye
absorption	17,600	4200	7.9
fluorescence	14,400	1360	3.0

and deuterated methanol (300 ps). The value in methanol was taken from Castner et al.,<sup>24</sup> and that for methanol-d<sub>4</sub> was calculated from the measured fluorescence yield,  $\varphi_f = \tau_f/\tau_{\text{rad}}$ , assuming the radiative lifetime  $\tau_{\text{rad}}$  is the same in both solvent isotopomers. The fluorescence lifetime and quantum yield for LDS750 in methanol imply a radiative lifetime of 58 ns compared with the value of 8.2 ns that we determined from the absorption and emission spectra using the Strickler–Berg equation.<sup>35</sup> The radiative rate is proportional to the square of the transition moment, which implies that the transition moment in the emitting state geometry is reduced from that at the Franck–Condon geometry. As shown in Table 2, the transition moment  $\mu_{\text{ge}}$  was found from the integrated absorption to be 7.9 D (Debye), leading to the an estimate of  $\mu_{\text{ge}} = 3.0$  D for emission. The structure of LDS750 is typical of molecules that undergo TICT (twisted intramolecular charge transfer) state formation. It has been reported that the fluorescence lifetime of LDS750 increases with increasing solvent viscosity, which is indicative of excited-state isomerization.<sup>24</sup> This isomerization is apparently accompanied by a decrease in the transition moment for emission.

The fluorescence anisotropy was determined to be  $r = 0.11$ , to be independent of excitation wavelength in the range 458 to 568 nm, and to be the same in deuterio- and protio-methanol. This anisotropy was obtained from a measurement of the parallel ( $I_{\parallel}$ ) and perpendicularly ( $I_{\perp}$ ) polarized emission intensity,<sup>36</sup> using eq 1:

$$\tau = \frac{I_{\parallel} - I_{\perp}}{I_{\parallel} + 2I_{\perp}} \quad (1)$$

The anisotropy at time zero  $r_0$  can be estimated using the Perrin equation:  $r_0 = r(1 + \tau_f/\phi_{\text{rot}})$ , where  $\phi_{\text{rot}}$  is the rotational relaxation time of the chromophore. Lian et al.<sup>30</sup> reported  $\phi_{\text{rot}} = 300$  ps for LDS750 in benzonitrile. Assuming this value is proportional to the solvent viscosity, we estimate  $\phi$  to be ~135 ps in methanol, which leads to a calculated value of  $r_0$  of 0.30 using the Perrin equation. This value of  $r_0$  implies an angle of 24° between the absorption and emission transition moments, which would suggest that internal rotation *precedes* emission. This suggestion is hard to reconcile with the time-domain emission results. In addition, it is difficult to understand why the anisotropy is the same in both methanol-h<sub>4</sub> and methanol-d<sub>4</sub>, whereas the difference in fluorescence lifetimes implied by the measured quantum yields, taken with the Perrin equation, suggest that  $r$  should vary with solvent isotope. (The viscosity of deuterated methanol is expected to be ~5% higher than that of methanol,<sup>37</sup> and cannot account for the difference in lifetime.)

These observations suggest that the time-averaged anisotropy  $r$  is determined by excited-state isomerization, which leads to a change in direction of the transition moment in the molecule frame in addition to overall molecular rotation. The Perrin equation can be modified to account for the influence of isomerization along with overall rotation:

$$r_0 = r \left( 1 + \frac{\tau_f}{\phi_{\text{isom}}} + \frac{\tau_f}{\phi_{\text{rot}}} \right) \quad (2)$$

Because the fluorescence lifetime is proportional to viscosity,<sup>24</sup> we assume that the isomerization time  $\phi_{\text{isom}}$  in eq 2 is equivalent to the fluorescence lifetime  $\tau_f$ . This assumption leads to the calculated value of  $r_0$  equal to 0.4, and the same value is obtained for both solvent isotopomers within the error of the anisotropy measurement. A value of  $r_0 = 0.4$  indicates the absorption and emission transition moments are parallel. Thus, the isomerization process quenches the emission, consistent with the aforementioned conclusions concerning the decrease in the magnitude of the transition moment for emission compared with that for absorption. We conclude that the increased fluorescence yield in deuterated methanol results from a decrease in the rate of radiationless relaxation, a consequence of less favorable Franck–Condon factors for lower-frequency solvent accepting modes. A similar effect has been observed in measurements of the nonradiative relaxation of betaine-30, which was observed to be slower in deuterio-alcohols compared with protio-alcohols.<sup>22</sup>

The possible existence of rotational isomers in the ground electronic state could account for some of the width of the absorption spectrum, and it is possible that a narrower distribution of rotational isomers in the excited state results in decreased width of the fluorescence spectrum. However, we observed no dependence of the anisotropy on excitation wavelength, as might be expected if the absorption spectrum were inhomogeneously broadened due to conformational isomers.

**3.2. Resonance Raman Spectra of LDS750.** Resonance Raman spectra were excited at 457.9, 488.0, 501.8, and 514.5 nm, using the same concentration of LDS750 in methanol and deuterated methanol. To compare Raman intensities of the dye in the two solvents, it was necessary to (1) subtract the fluorescence background and (2) scale the data according to the inherent relative intensity of the two solvents. The fluorescence subtraction proved to be a delicate operation, because of the congestion of Raman peaks. Data at points free from Raman scattering were selected for fitting to a polynomial, and the same points were used in both solvents at all excitation wavelengths. Solvent Raman intensities were determined in binary mixtures with cyclohexane, using the 802 cm<sup>-1</sup> line as a reference. Cross-sections for the cyclohexane standard were taken from Trulson and Mathies,<sup>38</sup> using the  $A$ -term expression of eq 12 and the tabulated fitting parameters of that work. Relative Raman intensities of CH<sub>3</sub>OH and CD<sub>3</sub>OD were also checked by careful comparison of the neat solvents and found to be in good agreement with values determined using the cyclohexane internal standard. For the argon laser wavelengths used here (457.9, 488.0, 501.8, and 514.5 nm), the total Raman cross-sections  $\sigma_{\text{R}}$  for the 802 cm<sup>-1</sup> line of cyclohexane were taken<sup>38</sup> as 130, 97.5, 86.0, and 76.9  $\mu\text{barn}$ , respectively (1  $\mu\text{barn} = 10^{-30}$  cm<sup>2</sup>). Differential Raman cross-sections for polarized scattering,  $(d\sigma/d\Omega)_{\parallel}$  are related to the total Raman cross-section  $\sigma_{\text{R}}$  as follows:

$$\sigma_{\text{R}} = \frac{8\pi}{3} (1 + \rho) \left( \frac{d\sigma}{d\Omega} \right)_{\parallel} \quad (3)$$

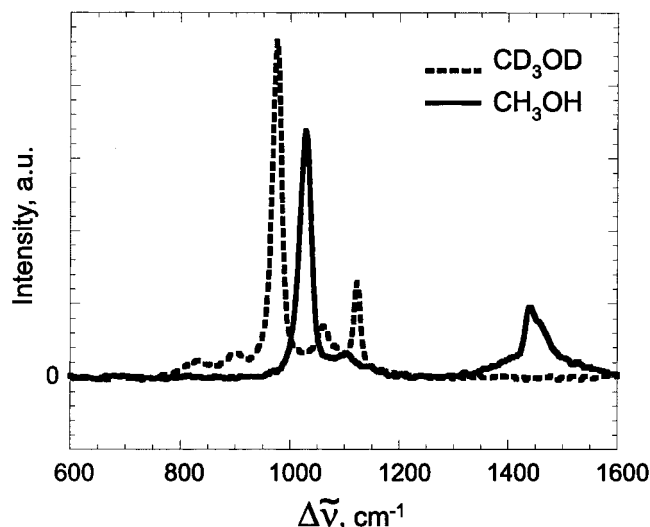


**Figure 3.** Raman spectra of CD<sub>3</sub>OD and CH<sub>3</sub>OH, excited at 514.5 nm and scaled to reflect relative Raman intensity.

**TABLE 3: Differential Raman Cross Sections, in  $\mu\text{barn}$ , of Methanol- $h_4$  and Methanol- $d_4$  for the Range 800–1200  $\text{cm}^{-1}$  and Peak Height Ratio as a Function of Excitation Wavelength  $\lambda_0$**

$\lambda_0$ , nm	$(d\sigma/d\Omega)_{\parallel}$ , CH <sub>3</sub> OH	$(d\sigma/d\Omega)_{\parallel}$ , CD <sub>3</sub> OD	$I_{978}/I_{1033}$
457.9	3.48	5.65	1.34
488.0	2.35	4.14	1.39
501.8	2.06	3.75	1.36
514.5	2.01	3.02	1.39

where  $\rho$  is the depolarization ratio. Relative intensities of Raman lines in the binary mixture are given by

$$\frac{I_1}{I_2} = \frac{N_1}{N_2} \frac{d\sigma_1/d\Omega}{d\sigma_2/d\Omega} \quad (4)$$

where  $N_i$  is the number density of component  $i$  and  $I_i$  is the area of the Raman band. Equations 3 and 4 were used to obtain the differential Raman cross-sections listed in Table 3. These values were integrated over the range 800–1200  $\text{cm}^{-1}$  to avoid errors in deconvoluting the main solvent lines, at 978  $\text{cm}^{-1}$  in CD<sub>3</sub>OD and 1033  $\text{cm}^{-1}$  in CH<sub>3</sub>OH, from nearby minor peaks. Peak height ratios for the main solvent bands were also determined and are listed in Table 3. Representative solvent Raman spectra are shown in Figure 3, scaled to reflect the relative intensities and corrected for instrument response. The refractive indices of CD<sub>3</sub>OD and CH<sub>3</sub>OH differ by <0.1%, so no local field correction was applied.

Figure 4 shows the polarized RR spectra of LDS750 in both solvent isotopomers, excited at 514.5 nm, after subtracting the fluorescence background. The spectra were scaled to give the same peak height ratio for the solvent lines as that given in Table 3. It is apparent that the LDS750 Raman intensities are the same, within error, in the two solvent isotopomers. The additional intensity in CH<sub>3</sub>OH in the 1400–1450  $\text{cm}^{-1}$  region is due to Raman scattering by the solvent (see Figure 3). This result was verified by subtracting the neat solvent spectra. As a check on the background subtraction and peak height scaling, the relative area of the subtracted solvent intensities (i.e., methanol compared with deuterated methanol), in the range 800–1200  $\text{cm}^{-1}$  was determined and found to be within  $\sim 10\%$  of the value expected from the cross-section data. Minor peaks due to LDS750 in the 1000–1100  $\text{cm}^{-1}$  region contribute somewhat to this error. Similar results were obtained at other

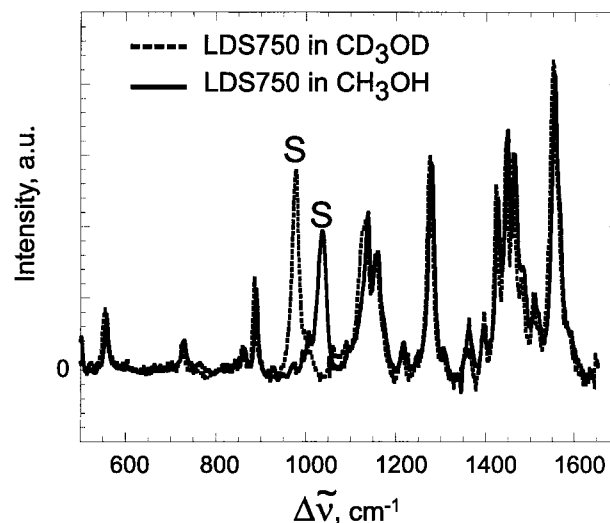


**Figure 4.** Resonance Raman spectra of LDS750 in CD<sub>3</sub>OD and CH<sub>3</sub>OH, excited at 514.5 nm and scaled to the relative Raman intensity of the solvent. Solvent lines are marked.

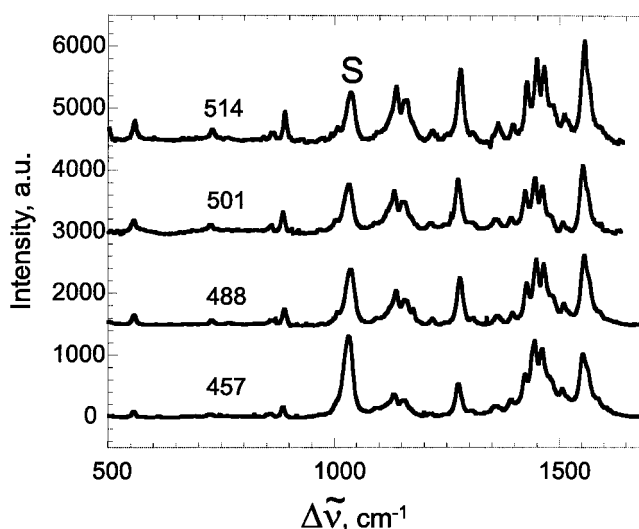


**Figure 5.** Resonance Raman spectra of LDS750 in CH<sub>3</sub>OH at four different excitation wavelengths, scaled to wavelength-dependent Raman intensity of solvent (S).

excitation wavelengths, though the Raman intensity of LDS750 compared with solvent decreases at shorter wavelengths, as shown in Figure 5. No obvious changes in the relative RR intensities of the dye were observed on comparing data in methanol and deuterated methanol.

The RR spectrum of LDS750 in CH<sub>3</sub>OH at 514.5 nm was previously reported by Bardeen et al.<sup>31</sup> Our results are comparable to theirs except we were unable to record Raman lines at wavenumber shifts lower than  $\sim 500$   $\text{cm}^{-1}$  because of limitations of our single monochromator. Raman spectra of LDS750 in CH<sub>3</sub>OH at various excitation wavelengths are shown in Figure 5.

#### 4. Discussion

Resonance Raman intensities of LDS750 in methanol and deuterated methanol were found to be the same within the error of the measurement, whereas fluorescence intensity is  $\sim 30\%$  greater in deuterated solvent. RR intensities are a sensitive function of the dephasing rate. In principle, this dephasing may contain contributions from population relaxation, but for the present system, the lifetime of 200–300 ps far exceeds the

Raman time-scale, so that the RR intensity is decided by pure dephasing (fluctuations in the transition frequency). In our previous studies of the solvatochromic dye betaine-30,<sup>11,12</sup> it was apparent that solvent-induced dephasing exerts a strong influence on the RR intensities. In the slow-modulation limit, where the amplitude of solvent-induced dephasing is large compared with the rate, the effect of increasing amplitude of solvent motion is to broaden the absorption spectrum and decrease the Raman intensities. Low-frequency intramolecular vibrations, such as internal rotation, can also induce pure dephasing, and the results of this study suggest that this sort of process overwhelms the effects of solvent-induced dephasing in the case of LDS750. This conclusion is in agreement with the results from time-domain measurements,<sup>31</sup> where a fast dephasing process was determined to be independent of solvent.

Though the lack of mirror symmetry of the absorption and emission spectra could indicate overlapping electronic transitions in the former, the depolarization ratios we observed suggest, but do not prove, that the visible absorption spectrum results from a single electronic transition. The femtosecond Stokes shifts study of LDS750 reported by Kovalenko et al.<sup>29</sup> suggest that the excited-state dynamics reflect isomerization, rather than internal conversion, and oscillations at a frequency of 173 cm<sup>-1</sup> were reported. The difference in the absorption and emission widths thus reflects the difference in the internal and/or solvent reorganization energies that influence absorption and emission. Low-frequency intramolecular motions can masquerade as solvent reorganization through the effect on the absorption spectra and Raman intensities. Both internal reorganization ( $\lambda_{\text{int}}$ ) and solvent reorganization ( $\lambda_{\text{solv}}$ ) contribute to the absorption and emission line width and the Stokes shift. For nonlinear solvent relaxation, the solvent response depends on the electronic state of the chromophore. Certainly, internal rotation can cause  $\lambda_{\text{int}}$  to differ for absorption and emission. Using single primes for ground-state quantities and double primes for excited-state properties, the absorption and emission maxima are

$$\tilde{\nu}_{\text{max,abs}} = E_0 + \lambda''_{\text{int}} + \lambda''_{\text{solv}} \quad (5)$$

$$\tilde{\nu}_{\text{max,fluor}} = E_0 + \lambda'_{\text{int}} + \lambda'_{\text{solv}} \quad (6)$$

The weak solvent dependence of the width and position of the fluorescence<sup>24</sup> indicates that  $\lambda'_{\text{solv}}$  is small. LDS750 is not soluble in nonpolar solvents, so we attempted to estimate the internal reorganization energy  $\lambda''_{\text{int}}$  from the dependence of  $\tilde{\nu}_{\text{max,abs}}$  on the solvent polarity according to the Lippert–Mataga equation:

$$\lambda_{\text{solv}} = \frac{\Delta\mu^2}{cha^3} \left[ \frac{\epsilon - 1}{2\epsilon + 1} - \frac{n^2 - 1}{2n^2 + 1} \right] \quad (7)$$

where  $\Delta\mu$  is the difference in the ground- and excited-state dipole moments,  $a$  is the Onsager cavity radius,  $\epsilon$  is the static dielectric constant, and  $n$  is the refractive index. The absorption maxima in a range of solvents, taken from Castner et al.,<sup>24</sup> were graphed versus the quantity in square brackets in eq 7. The intercept of 17 200 cm<sup>-1</sup> was taken as a crude estimate of  $E_0 + \lambda''_{\text{int}}$  and used to obtain a value of 1900 cm<sup>-1</sup> for the internal reorganization energy  $\lambda''_{\text{int}}$  and the value 400 cm<sup>-1</sup> for  $\lambda''_{\text{solv}}$ . Using eq 6, the total reorganization energy for emission must be  $\sim 900$  cm<sup>-1</sup>, which is considerably less than the value of 2300 cm<sup>-1</sup> for the total reorganization energy in absorption. Thus it is clear that the internal and solvent reorganization energies are different for the ground and excited states, as would be expected for a molecule that undergoes large structural rearrangement in the excited state.

The LDS750 molecule bears some similarity to the hemicyanine dye 4-[2-(4-dimethylaminophenyl)ethenyl]-1-methylpyridinium (HR), which we studied previously.<sup>13,14</sup> In that system, excited-state isomerization leads to a relaxed excited state with a charge distribution similar to the ground state, resulting in a much smaller  $\lambda_{\text{solv}}$  for emission than for absorption and weak dependence of the fluorescence spectrum on solvent polarity. Semiempirical calculations were employed to conclude that TICT state formation is associated with internal rotation about the single bond between the dimethylaniline group and the central double bond. It has been suggested<sup>24,29</sup> that in LDS750, internal rotation takes place about a single bond in the central butadiene part of the molecule. This solvent-dependent isomerization process takes place on a time scale of  $> 100$  ps, too long to influence the RR intensity. Internal rotation is expected to lead to a change in the direction of the transition moment, which is assumed to point from the dimethylamino electron donor group to the benzothiazolium acceptor. A shorter time scale (subpicosecond) intramolecular relaxation process has also been reported,<sup>29</sup> where it was concluded that this faster process of LDS750, rather than solvation, is responsible for the observed femtosecond Stokes shift. This putative isomerization takes place on a time scale of 200 fs in acetonitrile and 600 fs in chloroform, time scales relevant to resonance Raman scattering. Bardeen et al.<sup>31</sup> also attributed a sub-100 fs dephasing of LDS750 in methanol to an intramolecular relaxation. The absence of a solvent isotope effect on the Raman intensity supports this conclusion. Note that there is no change in the absorption spectrum of LDS750 after exposure to laser radiation; thus, the molecule returns to its original conformation in the ground state, and this internal process must contribute to the reorganization energy in both the absorption and emission spectra.

If solvent reorganization makes a negligible contribution to the fluorescence spectrum, then one must ask why the fluorescence yield (but not the anisotropy) should depend on solvent isotopomer. This question is particularly interesting considering there is no evidence for solvent–solute hydrogen bonding in this system; for example, a graph of absorption maximum versus the  $\pi^*$  solvent polarity scale does not distinguish protic from aprotic solvents.<sup>24</sup> The solvent reorganization energy, however, reflects the influence of the solvent on the ground- and excited-state energies of the chromophore, whereas the Franck–Condon factors for solvent acceptor modes in radiationless decay depend on the effect of the chromophore on the solvent vibrational modes. Some of these solvent modes are apparently displaced between the ground and excited states of the dye, in accord with the observation of Lian et al.,<sup>30</sup> who recorded transient changes in the solvent IR spectra following electronic excitation of LDS750. These changes were attributed to the large dipole moment change of LDS750 and the resulting difference in the local field experienced by molecules in the first solvation sphere. Though these displaced solvent modes are in principle coupled to the electronic transition, their enhancement in the RR spectrum would be difficult to observe due to the overwhelming response from unperturbed bulk solvent molecules.

## 5. Conclusions

The absence of a solvent isotope effect on RR intensities of LDS750 in methanol supports the idea that the sub-100 fs relaxation is due to intramolecular relaxation rather than solvent dynamics. The steady-state fluorescence spectrum, on the other hand, reveals emission from a relaxed excited state that has isomerized on a much longer ( $> 200$  ps) time scale. The

electronic transition moment of the relaxed state is decreased from the value at the Franck–Condon geometry, and internal rotation contributes to the steady-state fluorescence anisotropy. The observed solvent isotope effect on the fluorescence quantum yield derives from the solvent-dependent rate of radiationless relaxation.

More insight into the intramolecular processes responsible for excited-state relaxation in LDS750 is called for, but the task is made difficult by the large size of the molecule and uncertain contribution of rotational isomers in the ground electronic state. Nevertheless, it is clear that solvent isotope studies can help to distinguish between solvent and internal reorganization and thus contribute to improved methods for disentangling these effects in both time- and frequency-domain spectroscopy.

**Acknowledgment.** The support of the National Science Foundation is gratefully acknowledged.

### References and Notes

- (1) Maroncelli, M.; Fleming, G. R. *J. Chem. Phys.* **1987**, *86*, 6221.
- (2) Castner, E. W., Jr.; Maroncelli, M.; Fleming, G. R. *J. Phys. Chem.* **1995**, *99*, 17311.
- (3) Chang, Y. J.; Castner, E. W., Jr. *J. Phys. Chem.* **1996**, *100*, 3330.
- (4) Fleming, G. R.; Cho, M. *Annu. Rev. Phys. Chem.* **1996**, *47*, 109.
- (5) de Boeij, W. P.; Pshenichnikov, M. S.; Wiersma, D. A. *Annu. Rev. Phys. Chem.* **1998**, *49*, 99.
- (6) Castner, E. W., Jr.; Maroncelli, M. *J. Mol. Liq.* **1998**, *77*, 1.
- (7) Zusman, L. D. *Chem. Phys.* **1980**, *49*, 295.
- (8) Sumi, H.; Marcus, R. A. *J. Chem. Phys.* **1986**, *84*, 4272.
- (9) Walker, G. C.; Akesson, E.; Johnson, A. E.; Levinger, N. E.; Barbara, P. F. *J. Phys. Chem.* **1992**, *96*, 3728.
- (10) Cho, M.; Fleming, G. R. *Adv. Chem. Phys.* **1999**, *107*, 311.
- (11) Zong, Y.; McHale, J. L. *J. Chem. Phys.* **1997**, *106*, 4963.
- (12) Zong, Y.; McHale, J. L. *J. Chem. Phys.* **1997**, *107*, 2920.
- (13) Cao, X.; McHale, J. L. *J. Chem. Phys.* **1998**, *109*, 1901.
- (14) Cao, X.; Tolbert, R. W.; McHale, J. L.; Edwards, W. D. *J. Phys. Chem.* **1998**, *102*, 2739.
- (15) Albrecht, A. C. *J. Chem. Phys.* **1961**, *34*, 1476.
- (16) Stallard, B. R.; Champion, P. M.; Callis, P. R.; Albrecht, A. C. *J. Chem. Phys.* **1983**, *78*, 712.
- (17) Lee, S.-Y.; Heller, E. J. *J. Chem. Phys.* **1979**, *71*, 4777.
- (18) Heller, E. J.; Sundberg, R. L.; Tannor, D. *J. Phys. Chem.* **1982**, *86*, 1822.
- (19) Heller, E. J. *Acc. Chem. Res.* **1981**, *14*, 368.
- (20) Tannor, D. J.; Heller, E. J. *J. Chem. Phys.* **1982**, *77*, 202.
- (21) Reichardt, C. *Chem. Rev.* **1994**, *92*, 2319.
- (22) Reid, P. J.; Barbara, P. F. *J. Phys. Chem.* **1995**, *99*, 3554.
- (23) Pal, H.; Nagasawa, Y.; Tominga, K.; Kumazaki, S.; Yoshihara, K. *J. Chem. Phys.* **1995**, *102*, 7758.
- (24) Castner, E. W., Jr.; Maroncelli, M.; Fleming, G. R. *J. Chem. Phys.* **1987**, *86*, 1090.
- (25) Rosenthal, S. J.; Xie, X.; Du, M.; Fleming, G. R. *J. Chem. Phys.* **1991**, *95*, 4715.
- (26) Cho, M.; Rosenthal, S. J.; Scherer, N. F.; Ziegler, L. D. *J. Chem. Phys.* **1992**, *96*, 5033.
- (27) Goldberg, S. Y.; Bart, E.; Meltsin, A.; Fainberg, B. D.; Huppert, D. *Chem. Phys.* **1994**, *183*, 217.
- (28) Blanchard, G. J. *J. Chem. Phys.* **1991**, *95*, 6317.
- (29) Kovalenko, S. A.; Ernsting, N. P.; Ruthmann, J. *J. Chem. Phys.* **1997**, *106*, 3504.
- (30) Lian, T.; Kholodenko, Y.; Hochstrasser, R. M. *J. Phys. Chem.* **1995**, *99*, 2456.
- (31) Bardeen, C. J.; Rosenthal, S. J.; Shank, C. V. *J. Phys. Chem. A* **1999**, *103*, 10506.
- (32) Smith, N. A.; Meech, S. K.; Rubstov, I. V.; Yoshihara, K. *Chem. Phys. Lett.* **1999**, *303*, 209.
- (33) Book, L. D.; Scherer, N. F. *J. Chem. Phys.* **1999**, *111*, 792.
- (34) Eaton, D. F. *Pure Appl. Chem.* **1988**, *60*, 1107.
- (35) Strickler, S. J.; Berg, R. A. *J. Chem. Phys.* **1962**, *37*, 818.
- (36) Lakowicz, J. R. *Principles of Fluorescence Spectroscopy*; Plenum: New York, 1983.
- (37) Morresi, A.; Paliani, G.; Cataliotti, R. S. *J. Raman Spectrosc.* **1999**, *30*, 501.
- (38) Trulson, M. O.; Mathies, R. A. *J. Chem. Phys.* **1986**, *84*, 2068.